Supporting Information

Quantifying Risks of Asparagine Deamidation and Aspartate Isomerization in Biopharmaceuticals by Computing Reaction Free Energy Surfaces

*Nikolay V. Plotnikov, Satish Kumar Singh, Jason C. Rouse and Sandeep Kumar**

*Corresponding Author: Sandeep.Kumar@pfizer.com Tel: 636-329-2362

Proton transfer step and pH-dependence of the reaction rate

The reaction mechanism which involves an intramolecular proton transfer to the carbonyl oxygen of the Asn amide group or of the Asp carboxylate group is presented in **Figure 1** of the main text. The reaction rate can be described by the first order kinetics and is independent on pH:

$$-\frac{d[N]}{dt} = k_1[N] \qquad (S1)$$

Where [N] is the current concentration of reactants and k_1 is the reaction rate constant. An alternative mechanism is an intermolecular proton transfer (e.g. to OH^-):

$$> NH + HO^- \leftrightarrow > N^- + H_20$$

Here >NH symbolizes the backbone nitrogen of the n+1 residue, where n is the residue number of Asn or Asp in the protein structure. The reaction is described by the second order kinetics,

where the reaction rate depends on pH. At constant pH in buffer, $[HO^-]$ can be included in a pseudo first order constant $\tilde{k}_2$:

$$-\frac{d[N]}{dt} = k_2[N][HO^-] = \tilde{k}_2[N] \qquad (S2)$$

The reaction free energy for the proton transfer reaction ΔG°_{PT} is directly proportional to the difference in pKa between the donor and the conjugated acid of the acceptor (see **Table S2**). That is, for a series of proton acceptors A we can find the relative free energy of reaction, $\Delta\Delta G_{PT}$, using the proton transfer to OH^- as a reference:

$$\Delta\Delta G^\circ_{PT} = \Delta G^\circ_{PT,A} - \Delta G^\circ_{PT,OH} = RT\frac{(pK_{a,H2O} - pK_{a,A})}{\lg(e)} \qquad (S3)$$

The reaction free energy provides the lowest estimate for the free energy barrier for proton transfer reactions, with the upper estimate being 5 kcal/mol greater than the reaction free energy[1]. Potential proton acceptors and pKa's of their conjugate acids are listed in **Table S3**. Using **Eq. S3** we estimate the difference in the free energy barriers for proton transfer at 300 K, $\Delta\Delta g^\ddagger_{300}$. Furthermore, using **Eq. 2** of the main text we convert these free energy differences to corresponding ratios of the reaction rate constants. Finally, we can estimate the pH at which the reaction rate described by **Eq. S1** is equal to the reaction rate, described by **Eq. S2** (**Table S3**). While these estimates are very approximate, the difference in pKa between water and other acceptors makes the intramolecular proton transfer mechanism to the -CONH2 group of Asn very unlikely. The mechanism which involves proton transfer to the carboxylate group of Asp, however, can be competitive to proton transfer to OH^- at slightly acidic pH. As was pointed out in the main text, experimentally pH dependence was observed for Asn deamidation reactions while Asp isomerization demonstrates a rather weak pH dependence[2].

Experimental half-lives, rate constants and activation free energies

Integration of **Eq. S1** gives the concentration of Asn (or Asp) at time, t:

$$[N] = [N]_o \exp(-k_1 t) \quad (S4)$$

Where $[N]_0$ is the initial concentration. Using the definition of half-life ($\tau_{1/2}$) in **Eq. S4** we arrive to the equation which relates the half-life to the rate constant:

$$\frac{[N]_0}{2} = [N]_o \exp(-k\tau_{1/2}) \quad (S5)$$

Or:

$$\frac{ln2}{k} = \tau_{1/2} \quad (S6)$$

Therefore, the ratio of two rate constants is a reverse of the ratio of corresponding half-lives (compare to **Eq. 2** of the main text):

$$\frac{k_{PROT}}{k_{WAT}} = \frac{\tau_{1/2,WAT}}{\tau_{1/2,PROT}} \quad (S7)$$

For a given Asn site in a protein we are interested to know what is the ratio of the reaction rate constant at this site to the rate constant for Asn (or Asp) in GNG (or GDG) peptide in water. These peptides experimentally demonstrate the fastest degradation rates [2-3] and can serve as a convenient reference.

Supplementary information on calculations

Protein structures were prepared for molecular dynamics simulation using Molecular Operating Environment (MOE) [4]. Missing residues in crystal structures were built, protonation states for ionizable residues were determined at pH=6 and no salt and residues names were changed to Amber format during preparation in MOE. Proteins were neutralized and solvated with at least 10 Å of explicit TIP3P water using an octahedron for periodic boundary conditions with Amber tleap module. The system was energy minimized using MPI Sander module of

Amber, then it was heated to 300K and equilibrated in the NVT ensemble for 100 ps using 0.5 fs time steps. Afterward the system was pressurized to 1 bar and simulated in the NPT ensemble for 200 ps using 1 fs time steps followed by 600 ps using 2 fs timesteps. The final production run was 5 ns of NVT molecular dynamics with 2 fs time steps. Molecular dynamics simulations were performed using PMEMD GPU module of Amber. Amber14SB force field was used in these simulations. We used 8 Å cutoff, 2 fs integration time-steps with fixed bonds including hydrogen atoms. The production run was analyzed with the cpptraj module of Amber, and probability densities for χ and ψ dihedral angles were generated (**Figures S2-S4**).

A restart from the the production run was used in 4 independent PMF calculations for $N^{30}T$, $N^{55}G$, $D^{62}S$ and $D^{102}G$ sites. Each PMF calculation consisted of 73 trajectories propagated for 600 ps and biased to χ values from 0 to 360 in 5 degree increments. Only the last 300 ps were used in subsequent analysis to get values of χ every 20 fs. Those trajectories were run sequentially (on GTX TitanX or Nvidia Quadro M5000) toward 0 and toward 360 in parallel starting from the χ_0 closest to the χ value in the restart file. To check the convergence of calculations, the same protocol was repeated after hydrogen mass repartitioning (using Amber ParmEd module) with 4 fs time steps. Simulations of GDNF protein closely followed the protocol described above (for $D^{80}K$ and $D^{95}K$ sites in both monomers of the homodimer).

To simplify the QM/MM setup, we used the intramolecular proton transfer mechanism and the corresponding reaction coordinate [5] which involves proton transfer to the carbonyl oxygen of Asn or Asp (**Figure 1**). The proton transfer coordinate (d_{PT}) is the difference in distances between the carbonyl oxygen and the hydrogen of the backbone NH, and the hydrogen and the backbone nitrogen. The reaction coordinate component that describes the nucleophilic attack

(d_{NuA}) is the distance between the backbone nitrogen of n+1 residue and the C^{γ} atom of Asn or Asp. We constructed a 2D PM6/MM free energy surface for Asp isomerization at $D^{95}K$ site of GDNF (**Figure S5**) using the protocol described below. The minimum free energy path from this surface was represented by 33 points and used in all subsequent QM/MM free energy calculations.

Restart files for QM/MM calculation were taken from PMF calculations at χ_0 values corresponding to reactive conformations for $D^{102}G$, $N^{30}T$, $N^{55}G$, and $D^{62}S$ of trastuzumab and $D^{95}K$ of GDNF. For other potential degradation sites we didn't calculate the conformational PMF and we took the last frame from a 300 ps MD trajectory in NPT (after 700 ps in total) as restart files. Force constants used in all QM/MM algorithms were 250 kcal/(mol·Å^2). Once the bias on the reaction coordinate was introduced and the force-field was switched from MM to QM/MM we performed QM/MM energy minimization. Then, we sequentially run QM/MM NPT molecular dynamics (with velocity rescaling every 1 fs) for 1000 steps with 0.25 fs time step along the reaction path by gradually changing values for the bias potential. Next, for each QM/MM trajectory (each bias) we run an additional 1000 steps NPT MD (with velocity rescaling every 1 fs) with 0.25 fs time steps followed by 100000 steps NPT QM/MM MD with Langevin thermostat and 0.5 fs time steps.

QM/MM calculations reported in the main text were run using MPI-version of the Amber's Sander module after applying the truncation scheme given in **Figure S6**. We used the conventional electrostatic coupling scheme which is a default in Amber QM/MM: "All electrostatic interactions between all MM atoms (excluding MM atoms directly bonded to a QM atom) within the user specified cutoff distance of any QM atom are calculated for all QM atoms, including the link atom, without exclusion or scaling"[6]. We also tested different QM regions

shown in **Figure S7**. Thr, Ser and even Ile sidechain ($N^{30}T$, $D^{62}S$ and $N^{28}I$) which directly interact with the reaction center lower the free energy barrier when the n+1 sidechain is included in the QM region. These effects might be due to the charge transfer and induced polarization. Thr and Ser also formed a proton wire with the backbone nitrogen and the carbonyl oxygen of $-COO^-$ or $-CONH_2$, sometimes serving as intermediate proton acceptors. Another interesting effect of the QM region size was observed when the amide bond with the n+2 residue is included in the QM region. In such cases, QM/MM free energy calculations become QM size-dependent (**Figure S8**). The QM truncation scheme adopted in calculations of the main text ensures that all QM regions are of the same size.

We found that including the peptide bond with n+2 residue lowers the activation free energy by up to 14 kcal/mol (compare **Table 2** and **S4**). We also tried smaller QM regions without the n+2 peptide bond and without the sidechain of the n+1 residue (**Figure S8**). For some residues, N30T and N28I we encountered convergence issues in our algorithm when n+2 peptide bond was excluded and the n+1 sidechain included. In fact, we first computed the barrier with a small QM region without the side chain and without the n+2 peptide bond. Then we used the final restart files from those trajectories to compute the barrier for the final QM region shown in **Figure 6**.

Ace-GNG-Nme and Ace-GDG-Nme peptides were created and optimized by constraining ψ and χ dihedral angles to values in idealized reactive conformation (0° and -60°, and 180° and 60°), and by constraining ψ_2 to 0° or 180°. Then in QM/MM simulation a positional constraint with force constant of 5 kcal/(mol·Å^2) was applied to Nme and Ace residues. These constraints

are meant to define conformation of the NGN (compact versus extended) without explicitly biasing the dihedral angles. Nme is N-methylamine and Ace is acetyl.

Supplementary Tables

Table S1 Summary of experimental data on Asn deamidation and Asp isomerization.

	Initial degradation[1], %	Final degradation[2], %	Incubation pH and T/°K	Incubation time, days	$\tau_{1/2}/days$
Pentapeptide GGNGG	-	-	7.4 @ 310K	-	1 (Robinson et al.[3])
Pentapeptide GVNTG	-	-	7.4 @ 310K	-	50 (Robinson et al.[3])
Pentapeptide GFNIG	-	-	7.4 @ 310K	-	287 (Robinson et al.[3])
Hexapeptide VYPDGA	-	-	7.4 @ 310K	-	40 (Brennan et al. [2])
Trastuzumab $N^{30}T$ CDR1 V_L	11	24 (Sydow et al. [7])	6@ 313K	14	61
Trastuzumab $D^{102}G$ CDR3 V_H	7	22 (Sydow et al. [7])	6@ 313K	14	55
Trastuzumab $N^{55}G$ CDR2 V_H	4	5 (Sydow et al. [7])	6@ 313K	14	927
GDNF $D^{95}K$	0	5 (Hui et al. [8])	5@ 310K	7	95

[1]Unstressed sample; [2]Stressed sample, forced degradation

Table S2 Relationship between the acidity constants and the reaction free energies for proton transfer reactions. The reaction free energy for proton transfer is related to the difference between pKa of the donor and pKa of the conjugate acid of the acceptor.

Reaction	Equilibrium constant	Standard free energy
$> NH + H_2O \leftrightarrow > N^- + H_3O^+$	$K_{a,1} = \frac{[H^+][> N^-]}{[> NH]}$	$\Delta G^\circ = RT\frac{pK_{a,1}}{\lg(e)}$
$HA + H_2O \leftrightarrow A^- + H_3O^+$	$K_{a,2} = \frac{[H^+][A^-]}{[HA]}$	$\Delta G^\circ = RT\frac{pK_{a,2}}{\lg(e)}$
$> NH + A^- \leftrightarrow > N^- + HA$	$K = \frac{K_{a,1}}{K_{a,2}}$	$\Delta G^\circ_{PT} = RT\frac{(pK_{a,1} - pK_{a,2})}{\lg(e)}$

Table S3 Comparison of pKa for conjugated acids of potential proton acceptors. 3rd and 4th columns show differences in activation free energies relative to the proton transfer to hydroxyl anion. The 5th column shows the ratio of the rate constants that corresponds to the activation free energy difference. The last column is the pH at which the rate constant for the intramolecular proton transfer is equal to the pseudo-first order rate constant for the proton transfer to hydroxyl anion. The error is estimated for one unit in pKa uncertainty.

Proton acceptor	pKa conj. acid	$\Delta\Delta g^{\ddagger}_{300}$ /(kcal/mol)	$\Delta\Delta g^{\ddagger}_{310}$ /(kcal/mol)	k_{OH}/k_A	pH:$k_1 = \tilde{k}_2$
OH^-	15.7±1	0±1.4	0±1.4	1	
$-COO^-$ (Asp)	3.8±1	16.3±1.4	16.9±1.4	7.9E11±1	2.1±1
$MeC(NMe_2)O$	-0.2±1	21.8±1.4	22.6±1.4	7.9E15±1	-1.9±1
H_2O	-1.7±1	23.9±1.4	24.7±1.4	2.5E17±1	-3.4±1

Table S4 Results from additional calculations exploring the effect of the QM region size on QM/MM free energy calculations. Small and big QM regions are defined as CH_3-CO-NH-$CH(CH_2COX)$-CO-NH-CH_3 and CH_3-CO-NH-$CH(CH_2COX)$-CO-NH-CH(R)-CO-NH-CH_3, where X=NH_2 or O^- and R is the n+1 side chain. "No" or "with" followed by the residue name indicate that big or small QM region is modified by excluding or including the n+1 side chain.

	QM region	$^1\Delta g^{\ddagger}$	$^1\Delta G_r$	$^{1,2}\Delta\Delta g^{\ddagger}$	$^{1,2}\Delta\Delta G_r$
Ace-GNG-Nme $^3RC_1$ $^3RC_2$ $^3RC_3$ $^3RC_4$ Average	small QM	 37.1 36.1 38.2 37.8 37.1	 4.1 3.8 6.2 3.9 2.3	 reference	 reference
Trastuzumab $N^{55}G.V_H$	small QM	39.1	9.3	$2+^4 0.8$	$5.2+^4 0.8$
Trastuzumab $N^{30}T.V_L$	small QM	45.7	7.3	8.6	3.2
Trastuzumab $N^{28}I.V_H$	small QM	53.0	23.7	15.9	19.6
Ace-GDG-Nme $^3RC_1$ $^3RC_3$ Average	small QM	 28.0 27.8 27.9	 8.9 7.7 8.8	 reference	 reference
Peptide SDK	small QM with Lys	28.9	8.5	1.0	-0.3
GDNF $D^{95}K$	small QM with Lys	34.6	18.5	$6.7+^4 0.9$	$9.7+^4 0.9$
Trastuzumab $D^{102}G.V_H$	small QM	33.7	15.9	5.8	7.1
Trastuzumab $D^{62}S.V_H$	small QM	37.1	21.5	$9.2+^4 1.8$	$12.7+^4 1.8$
Trastuzumab $D^{31}T.V_H$	small QM with Thr	39.3	26.1	11.4	17.3
Trastuzumab $D^{28}V.V_L$	small QM with Val	39.6	22.3	11.7	13.5
Trastuzumab $D^{108}Y.V_H$	small QM with Tyr	41.4	25.0	13.5	16.2
Ace-GNG-Nme $^3RC_1$	big QM	 30.5	 4.6		

$^3RC_2$ $^3RC_3$ $^3RC_4$ Average		28.4 29.2 29.4 29.4	3.1 5.9 3.6 4.3	reference	reference
Trastuzumab $N^{30}T.V_L$	big QM	32.9	10.7	3.5	6.4
Trastuzumab $N^{30}T.V_L$	big QM no Thr	36.4	6.6	7.0	2.3
Trastuzumab $N^{55}G.V_H$	big QM	35.1	12.7	5.7+[4]0.8	8.4+[4]0.8
Trastuzumab $N^{28}I.V_H$	big QM	38.2	12.9	8.8	8.6
Trastuzumab $N^{28}I.V_H$	big QM no Ile	37.7	14.8	8.3	10.5
Ace-GDG-Nme $^3RC_2$ $^3RC_4$ Average	big QM	 20.1 22.6 21.4	 3.8 5.8 4.8	reference	reference
GDNF $D^{95}K$	big QM no Lys	26.1	11.6	4.7+0.9	6.8+0.9
Trastuzumab $D^{102}G.V_H$	big QM	27.3	13.6	5.9	8.8
Trastuzumab $D^{62}S.V_H$	big QM no Ser	26.3	16.1	4.9+1.8	11.3+1.8
Trastuzumab $D^{31}T.V_H$	big QM no Thr	33.0	22.5	11.6	17.7
Trastuzumab $D^{28}V.V_L$	big QM no Val	35.1	22.2	13.7	17.4
Trastuzumab $D^{108}Y.V_H$	big QM no Tyr	33.8	23.9	12.4	19.1
GDNF $D^{95}K$	big QM	27.2	13.7	5.8+0.9	8.9+0.9
Trastuzumab $D^{62}S.V_H$	big QM	22.3	11.8	0.9+1.8	7+1.8
Trastuzumab $D^{31}T.V_H$	big QM	25.7	15.5	4.3	10.7
Trastuzumab $D^{28}V.V_L$	big QM	31.6	17.2	10.2	12.4
Trastuzumab $D^{108}Y.V_H$	big QM	31.7	20.1	10.3	15.3

[1]values are in kcal/mol; color legend using arbitrary cut off consistent with experimental data: red – high risk, yellow – moderate risk, green – low risk; entries highlighted in yellow are false-predictions obtained with the QM model that includes the n+1 side chain.

[2]relative values to the peptide in water with the same QM region

[3]Reactive Conformations. RC_1: ψ_1~180˚ ψ_2~0˚ χ~60˚; RC_2: ψ_1~0˚ ψ_2~0˚ χ~-60˚; RC_3: ψ_1~180˚ ψ_2~180˚χ~60˚; RC_4: ψ_1~0˚ ψ_2~180˚ χ~-60˚

[4]The reaction free energy profile is elevated by the free energy of moving to reactive conformation, ΔG_{CONF}

Supplementary Figures

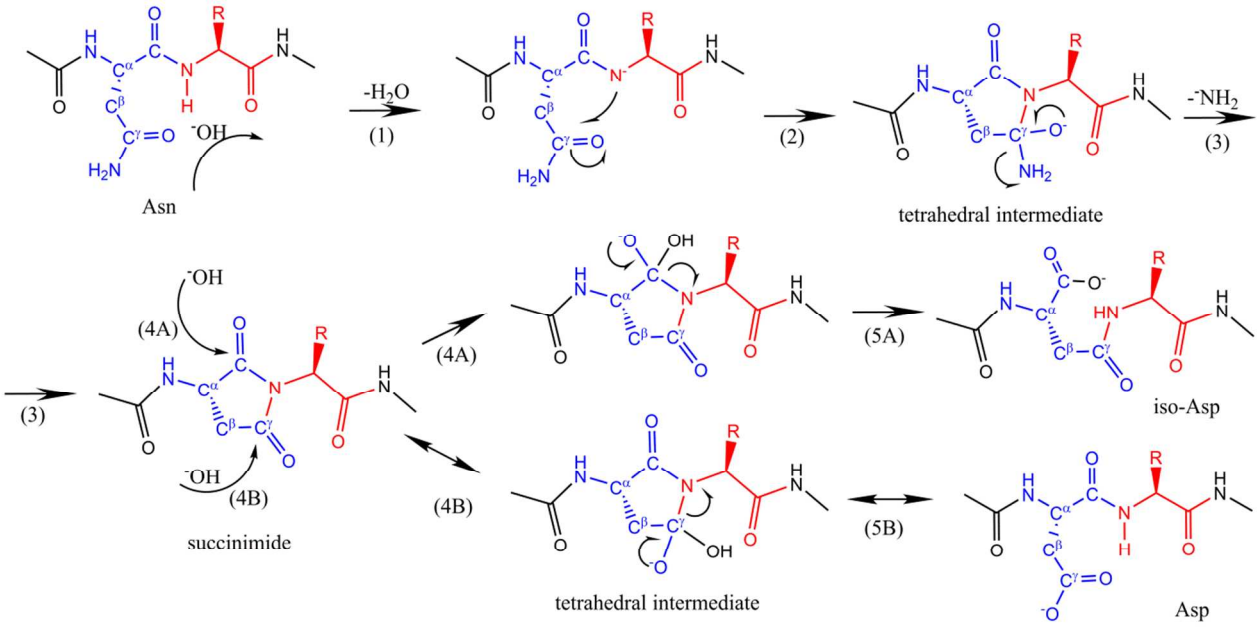

Figure S1 Scheme demonstrating reaction mechanism for Asn deamidation. (1) Ionization of the backbone nitrogen of the n+1 residue by a hydroxyl anion creates a strong nucleophile (2) The nucleophilic nitrogen attacks the C^{γ} carbon yielding the tetrahedral intermediate (3) The tetrahedral intermediate loses the $-NH_2$ group and converts to succinimide. (4) Succinimide undergoes hydrolysis under basic conditions. Depending on which electrophilic center is attacked, this step results in formation of iso-Asp (A) or Asp (B). Step 5B and 4B are reversible and describe succinimide-mediated isomerization of Asp.

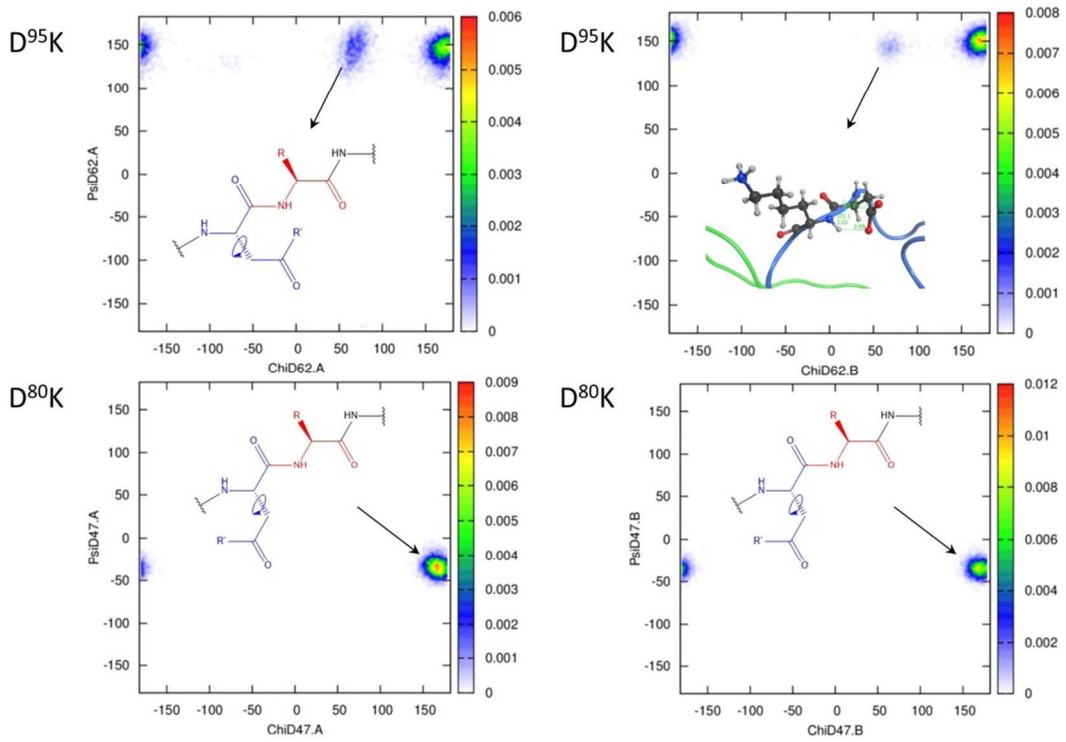

Figure S2 Probability density maps for ψ and χ dihedral angles computed from a 5 ns MD trajectory. The top two panels are for $D^{95}K$ site in GDNF which is known to degrade experimentally, while the two bottom panels are for $D^{80}K$, chemically stable sites. Arrows indicate reactive conformation (top) visited by degradable sites and non-reactive conformation.

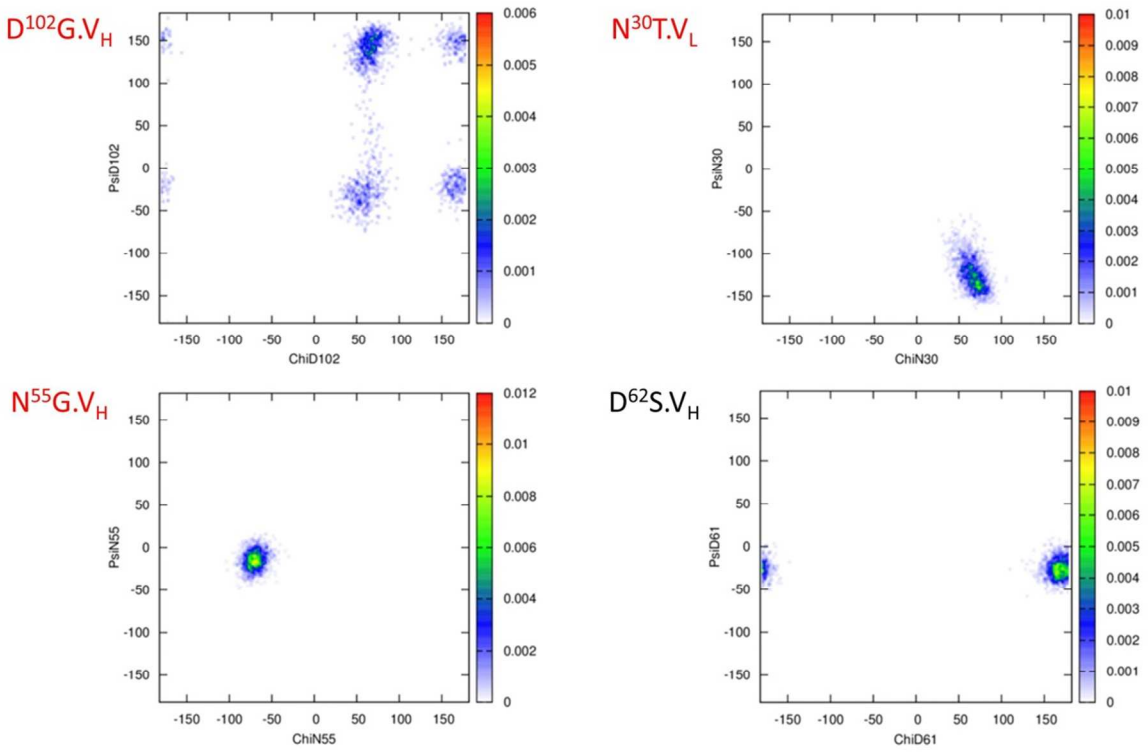

Figure S3 Probability densities for ψ and χ dihedral angles computed from a 5 ns MD trajectory. The panels are for (clockwise starting from the top left corner): $D^{102}G$ of V_H, $N^{30}T$ of V_L, $N^{55}G$ of V_H and $D^{62}S$ of V_H. All sites except the $D^{62}S$ are known to degrade experimentally [7]. All sites are found in or near reactive conformations in the crystal structure (PDB ID 1N8Z) as given in **Table 1** of the main text.

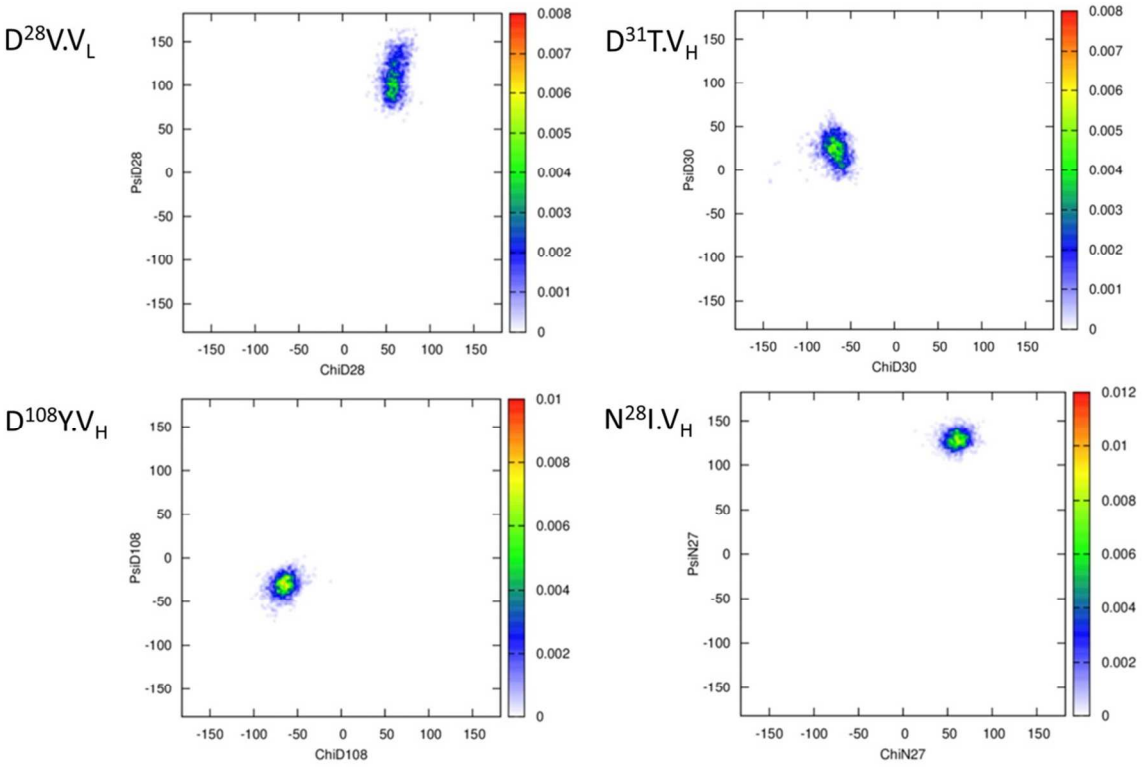

Figure S4 Probability densities for ψ and χ dihedral angles computed from a 5 ns MD trajectory. The panels are for (clockwise starting from the top left corner): $D^{28}V$ of V_L, $D^{31}T$ of V_H, $D^{108}Y$ of V_H and $N^{28}I$ of V_H. Interestingly, all sites are known to be stable experimentally, however they are found in reactive conformations either at ψ~180° and χ~60° (DV, NI) or at ψ~° and χ~-60° (DY, DT), see also **Table 1** of the main text.

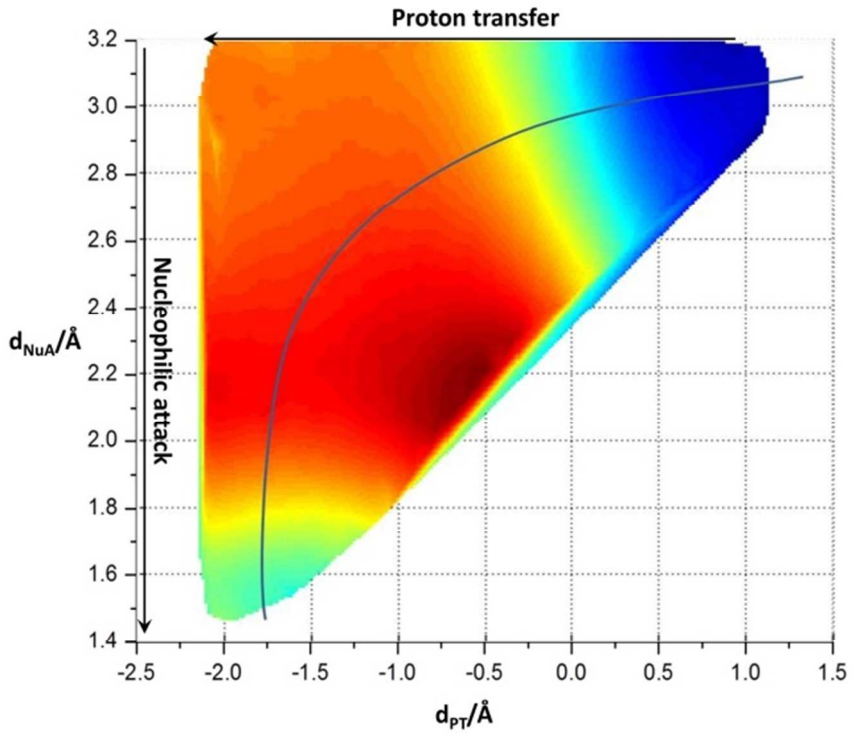

Figure S5 PM6/MM free energy surface for the chemical step in $D^{95}K$ degradation hotspot of GDNF protein. QM region includes backbone atoms between C^{α} carbons or n-1 and n+1 residues and sidechains of Aps and of Lys residues, where n is the number of Asp. The least free energy path is shown with a blue line. Values of the reaction coordinate (in Å) used for the free energy path: ($\mathbf{d_{PT}}$, $\mathbf{d_{NuA}}$)=(1.36, 3.11; 1.22, 3.09; 1.11, 3.07; 0.95, 3.07; 0.8, 3.05; 0.61, 3.04; 0.44, 3.03; 0.28, 3.01; 0.15, 3; 0.01, 2.98; -0.13, 2.95; -0.25, 2.94; -0.38, 2.92; -0.52 , 2.88; -0.65, 2.85; -0.77, 2.81; -0.91, 2.77; -1.03, 2.73; -1.15, 2.67; -1.29, 2.61; -1.4, 2.56; -1.49, 2.49; -1.56, 2.41; -1.63, 2.33; -1.67, 2.26; -1.69, 2.19; -1.72, 2.11; -1.76, 2.02; -1.78, 1.93; -1.79, 1.84; -1.79, 1.74;-1.8, 1.66;-1.8, 1.57; -1.79, 1.49)

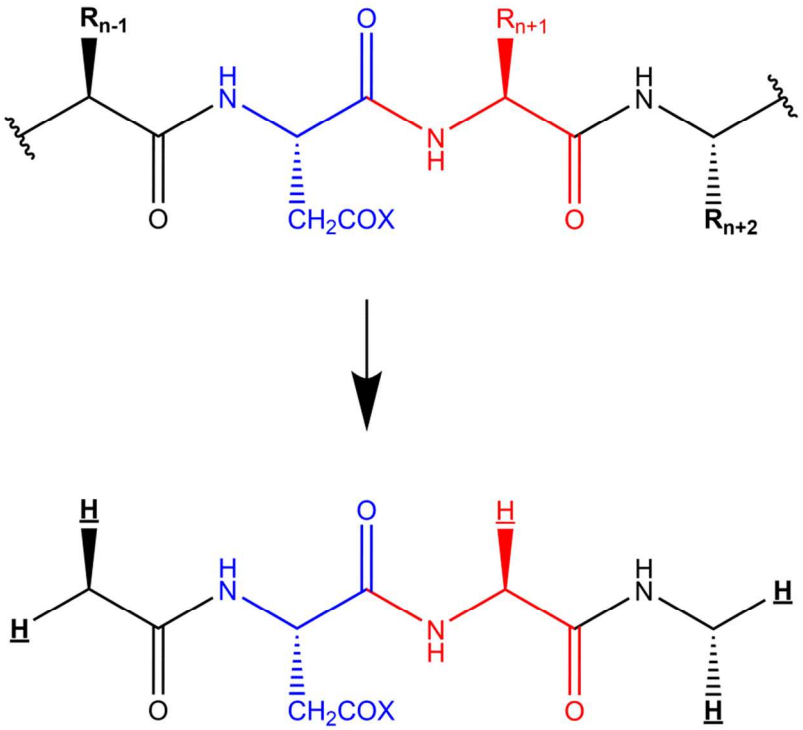

Figure S6 Transformation of a potential degradation site in protein (the upper image) to the QM region (the lower image) in the final QM/MM scheme. Incisions in the protein backbone are made to include C^{α} atoms of the n-1 and n+2 residues (shown in black), where n is Asn or Asp residue (which is shown in blue), and the n+1 residue (shown in red). Additional incisions are made to exclude side chains of n-1, n+1, and n+2 residues from the QM region. Open valences resulting from cutting bonds are capped with hydrogen link atoms, which are underlined in the bottom image. This protocol results in the QM region of the same size, which corresponds to GNG or GDG sequence motifs.

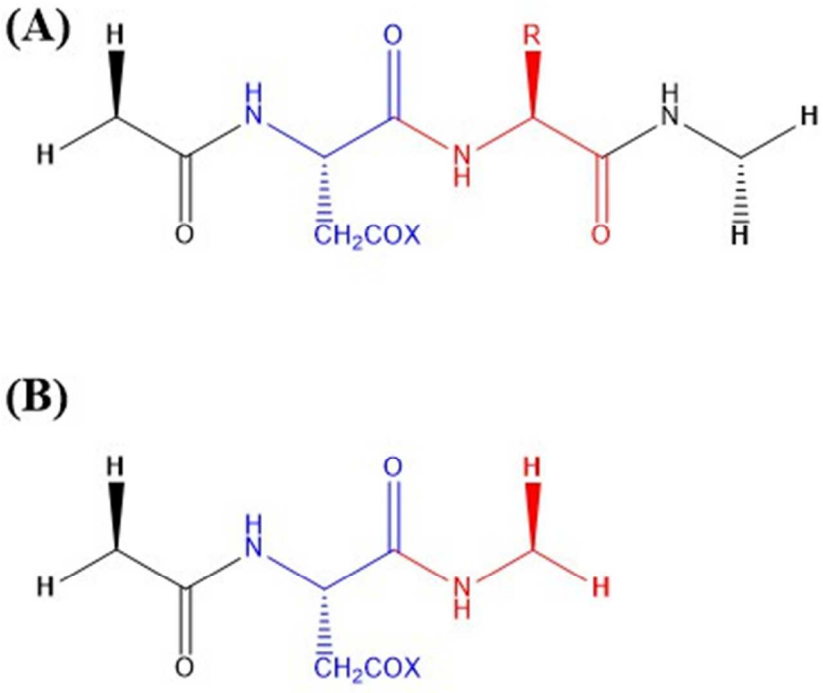

Figure S7 QM regions used in QM/MM calculations in this work: Asn or Asp is colored in blue, the n+1 residue is colored in red, H-linked atoms are shown in bold explicitly (A) represents an extended QM region while (B) represents a smaller QM model used in calculations in the main text. As pointed out in the main text, we do not include the n+1 side chain in the QM model in order to make a consistent comparison across degradation sites with different sequence motifs.

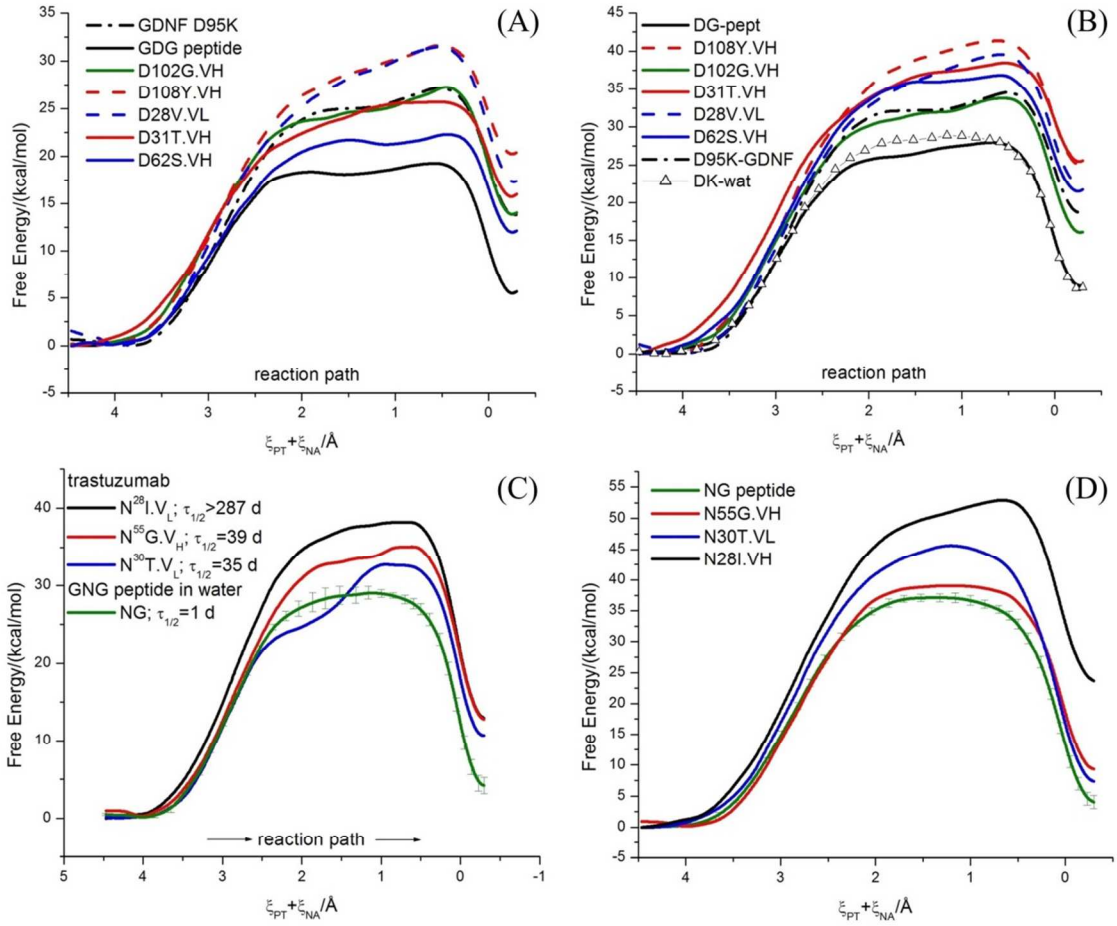

Figure S8 Free energy surfaces for the chemical step from reactive conformations provide estimates for the activation and reaction free energies. Using big QM region (A) Asp-isomerization in GDG peptide in water (black solid line); in the CDR of trastuzumab: $D^{102}G$ V_H (solid green), $D^{31}T$ of V_H (solid red), $D^{28}V$ of V_L (dashed blues) and $D^{108}Y$ of V_H (dashed red); in GDNF: $D^{95}K$ (dash-dot black). (B) Using small QM region with no peptide bond of the n+2 residue and no n+1 side-chain for $D^{62}S$, $N^{30}T$ and $N^{28}I$. (C)-(D) Asn-deamidation in GNG peptide in water (solid green averaged over 2 reactive conformations with extended and compact ψ_2); in the CDR of trastuzumab: $N^{55}G$ site of V_H (solid red), $N^{30}T$ of V_L (solid blue) and $N^{28}I$ of V_H (solid black).

References

1. Xiang, Y.; Warshel, A., Quantifying Free Energy Profiles of Proton Transfer Reactions in Solution and Proteins by Using a Diabatic FDFT Mapping. *The Journal of Physical Chemistry B* **2008,** *112* (3), 1007-1015.
2. Brennan, T.V.; Clarke, S., Spontaneous Degradation of Polypeptides at Aspartyl and Asparaginyl Residues: Effects of the Solvent Dielectric. *Protein Science* **1993,** *2* (3), 331-338.
3. Robinson, N.E.; Robinson, A.B., Molecular Clocks. *Proceedings of the National Academy of Sciences* **2001,** *98* (3), 944-949.
4. *Molecular Operating Environment (MOE)*, 2015; Chemical Computing Group Inc. : Montreal, QC, Canada, 2016.
5. Ugur, I., et al., Why Does Asn71 Deamidate Faster Than Asn15 in the Enzyme Triosephosphate Isomerase? Answers from Microsecond Molecular Dynamics Simulation and QM/MM Free Energy Calculations. *Biochemistry* **2015,** *54* (6), 1429-1439.
6. Walker, R.C., et al., The Implementation of a Fast and Accurate QM/MM Potential Method in Amber. *Journal of Computational Chemistry* **2008,** *29* (7), 1019-1031.
7. Sydow, J.F., et al., Structure-Based Prediction of Asparagine and Aspartate Degradation Sites in Antibody Variable Regions. *PLoS ONE* **2014,** *9* (6), e100736.
8. Hui, J.O., et al., Identification of Asp95as the Site of Succinimide Formation in Recombinant Human Glial Cell Line-Derived Neurotrophic Factor. *Archives of Biochemistry and Biophysics* **1998,** *358* (2), 377-384.